Pure & Appl. Chem., Vol.51, pp.731-745.
Pergamon Press Ltd. 1979. Printed in Great Britain.

0033-4545/79/0401-0731 $02.00/0

STUDIES ON SOME BIOLOGICALLY ACTIVE COMPOUNDS

Koji Nakanishi

Department of Chemistry, Columbia University, New York, N.Y.10027 USA

Abstract - The structures of a mitotic hormone that regulates cell proliferation, a 7,12-dimethylbenzanthracene guanosine adduct formed upon tissue culture and the neurotoxin neosaxitoxin are presented. The antisickling agent DBA has been shown to act by interacting with the binding of sickle cell hemoglobin to the membrane.

1. A mitotic hormone that regulates cell proliferation (Ref.1).

Eukaryotic cells proliferate according to the cycle shown in Fig.1. Namely, after mitosis, the cells proceed through a stage called gap-1 (G1); this is followed by a DNA synthetic stage in which the DNA content is doubled. The phase between the synthetic and mitotic stages is called gap-2 (G2). The search for natural substances that regulate the cell proliferative

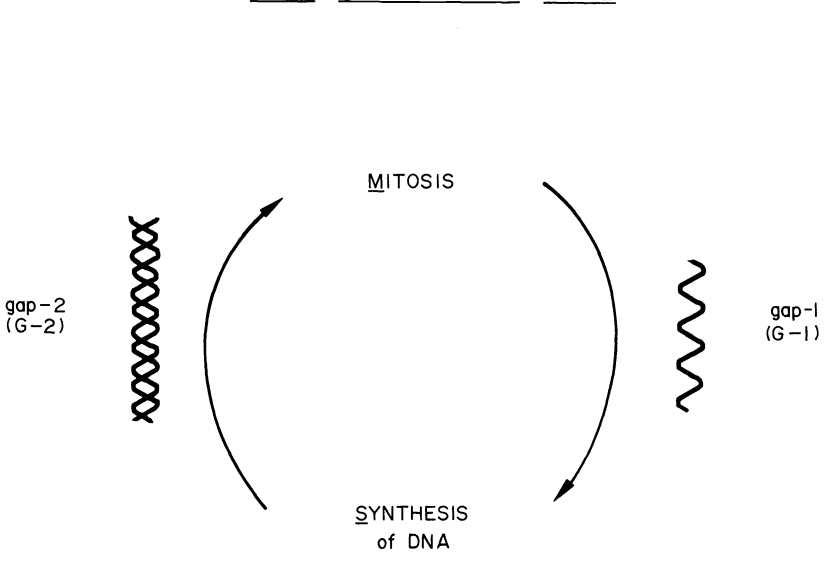

Fig. 1 Proliferation cycle

cycle, an important aspect in cancer research, were initiated by the discovery of chalones in the early 1960's (Refs.2,3). However, the chalones, a class of mammalian glycoproteins which arrest cell activity in either G1 or G2, are still uncharacterized.

Evans and Van't Hof discovered in 1972 that a so-called G2 factor present in cotyledons of garden peas (Pisum sativum) promotes cell arrest in the G2 stage of both roots and shoots (Ref.4).

Many of the physiological roles of the G2 factor resemble those of chalones. Normally cells deprived of an energy source will be arrested predominantly in the G1 stage, but with addition of the G2 factor a much higher percentage of cells are arrested in G2. Namely, when the meristematic tip cells of the peas are incubated in White's medium containing 2% sucrose, a continuous growth of the root takes place according to the M/G1/S/G2 proliferation cycle. However, when the energy source sucrose is deleted, the meristematic cells are arrested in G1 (80%) and G2 (20%) only, and no root growth is observed after 24 hours. Addition of G2 factor, on the other hand, promotes arrest in G2; thus addition of pure G2 resulted in 20% G1 and 80% G2.

The isolation was carried out according to Fig.2. Seeds of garden peas were surface-sterlized and germinated on sterile vermiculite. The cotyledons of 3 day-old seedling (ca.32,00) were excised and incubated for 2 days in 8 liters of sterile water in 160 culture flasks. The aqueous extract was filtered through a graded series of filters until it passed a 0.30 mesh

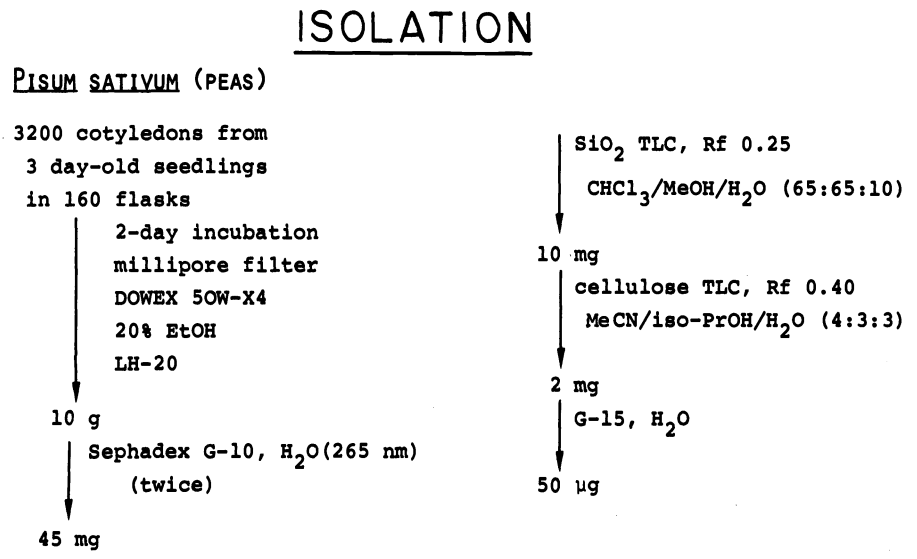

Fig. 2 Isolation scheme for the G2 factor

millipore filter, and then submitted to a series of chromatographies terminating with Sephadex G-15 gel filtration. Each fractionation was followed by bioassay until it was found that an absorption maximum of 265 nm was associated with the activity. The final yield was 50 µg of a hygroscopic polar compound which was insoluble in most organic solvents excepting MeOH and DMSO. The entire process was repeated 4 more times to give a total of 250 µg.

The FTIR showed (Fig.3) a series of well-defined bands. The bands at 1675, 1645, and 1620 cm^{-1} together with the 780 cm^{-1} suggested that some N-heteroaromatic nucleus (Ref.5) with probably three adjacent aromatic hydrogen atoms was present. The intense 1370 cm^{-1} band was confusing while the bands around 3400 cm^{-1} suggested that some hydroxylic function was present. The $^{+}$PMR (Fig.4), which was quite straightforward, consisted of bands due to a N^{+}Me group, a low-field singlet at 9.20 ppm and three other low-field signals, arising from three contiguous protons, i.e. 8.87 (d,6.5), 8.75 (d,7.5) and 8.20 ppm (dd, 6.5 and 7.5).

The UV (Fig.5) remained unchanged at pH 7 and above, but showed some fine structure when acidified. Due to insufficient volatility, the crucial molecular formula could not be obtained in spite of numerous attempts by various MS methods, i.e., chemical ionization, field desorption and electron impact MS. However, one particular 50 µg batch unexpectedly and fortunately gave the M^{+} peak in a trivial manner at a stage when attempts to measure the

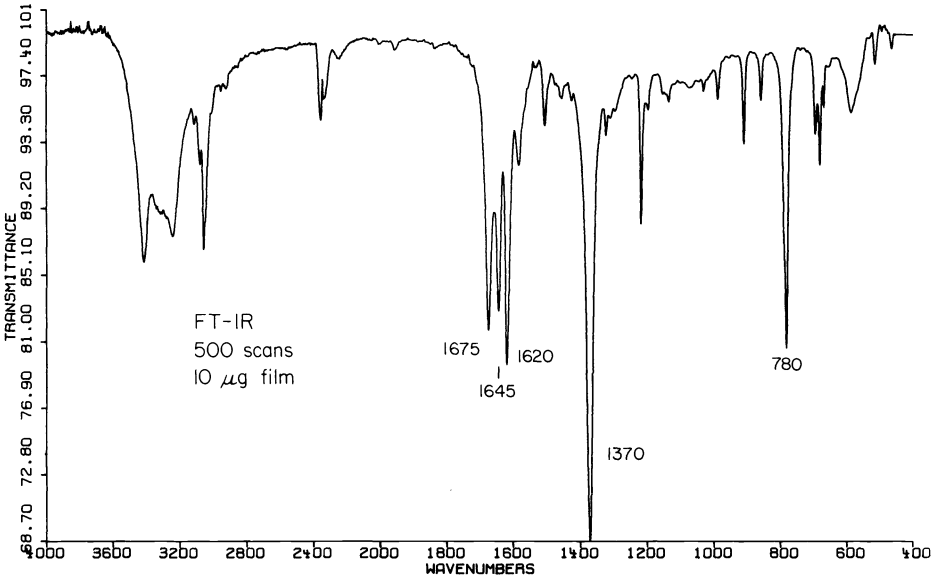

Fig.3. FTIR of G2 factor, KRS-5 plate (measured by Dr.G.Jordan, Nicolet, model 7199).

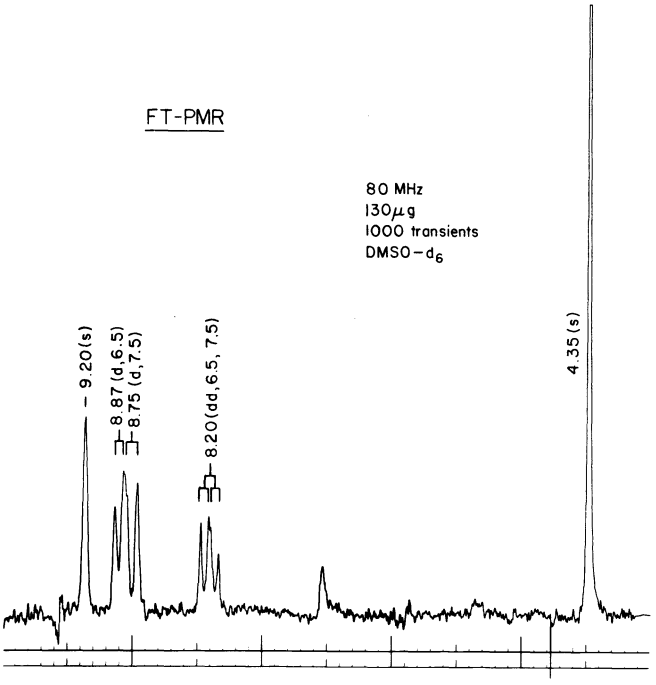

Fig.4. FT-PMR of G2 factor

MS were almost abandoned; high resolution results (Varian MAT 731) thus obtained are shown in Fig. 5. These MS data together with other spectroscopic data readily led to the structure of N-methylnictonic acid. Presumably the batch which gave the satisfactory MS data contained the protonated form as well as the zwitterionic form. The IR bands around 3400 cm^{-1} should now be assigned to absorbed moisture.

Finally a satisfactory 20 MHz CMR spectrum (Varian FT-80A,Fig.6) using the combined lots of sample was obtained using a 3 sec repetition time, 239,400 transients, which took 9 days. The 168.6 and 137.9 ppm peaks were

HIGH RESOLUTION EI-MS

VARIAN-MAT 731

190°, 70 eV

$C_7H_8NO_2$

139 (35%): M+1

138 (80%): M

123 (25%): M-CH_3

94 (100%): C_6H_8N, M-CO_2

79 (35%): C_5H_5N

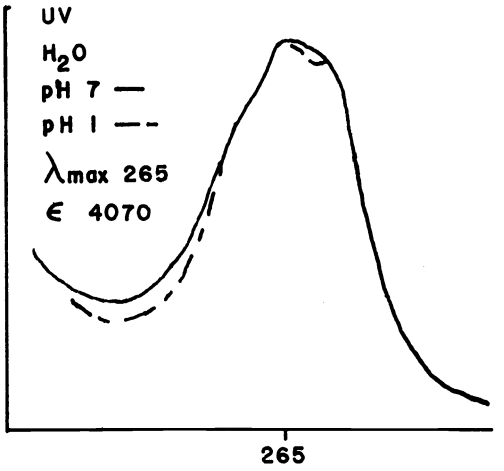

Fig.5. High resolution EI-MS and UV of G2 factor

absent in a 3-day run with a repetition time of 0.819 sec. thus identifying these peaks as being due to non-protonated carbons. The integrated peak heights (Fig.5,bottom) was of diagnositc value in making peak assignments since the peaks attached to the quaternary nitrogen, i.e., C-2, C-6 and Me, had wider half-band widths due to residual C-$^{14}N^+$ couplings. The conclusion that G2 was N-methylnicotinic acid was finally confirmed by comparison with authentic material.

N-Methylnicotinic acid or trigonelline (Ref.6) was indeed first isolated from Trigonella foenum-graecum in 1885 and already synthesized in 1886. It has since been isolated from any other sources. However, except for its role as a partial substitute for the vitamin nicotinic acid, no independent

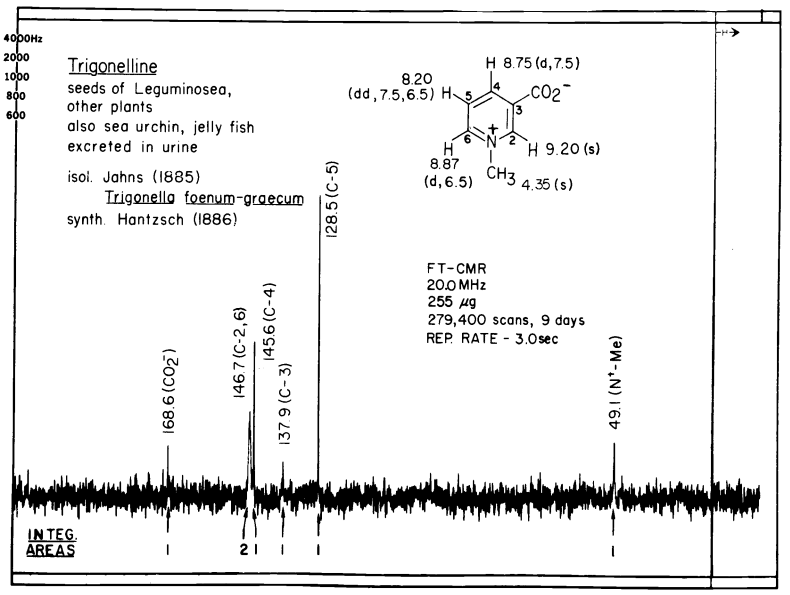

Fig.6. 20 MHz FT-CMR of G2 factor, 279,400 scans.

function had been assigned. Trigonelline is the first hormone to be characterized from plant or animal sources that regulates all proliferation by cell arrest in either G1 or G2 in complex tissues. It should also be noted that the cortex of legumes are preponderantly in G2 when nodules leading to nitrogen fixation, are formed. The mode of regulation of trigonelline in the cell cycle must await further investigations.

2. Structure of a 7,12-dimethylbenz[a]anthracene/nucleic acid adduct G*-II formed upon tissue culture with rat liver (Ref.7).

7,12-Dimethylbenz[a]anthracene (DMBA)-5,6-oxide has been implied as being one of the intermediates, but not the major (Ref.8), responsible for the carcinogenecity of DMBA. In 1976 we showed that reaction of the

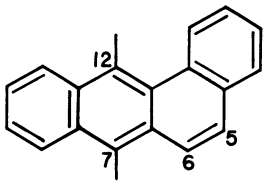

DMBA

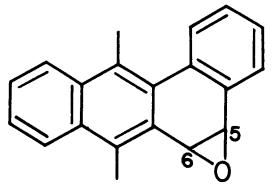

DMBA-5,6-oxide

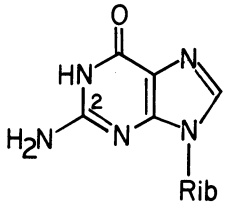

guanosine

Fig.7, DMBA, DMBA-5,6-oxide and guanosine

(±)-5,6-oxide with polyguanilic acid at pH in 50% aq. acetone led to four adducts resulting from the nucleophilic attack of N^2 of guanosine at carbons 5 and 6 (α- and β- attacks) of the 5,6-oxide with concommitant trans opening of the oxirane ring (Ref.9). However, since none of the four corresponded to the tissue culture products resulting from incubation of mouse skin and hamster or mouse embryo cells (Ref.10) another set of in vitro products were prepared at pH 9.5 and separated (Fig.8). Under these conditions 15% of the guanosine reacted to give six adducts G*-Ia, Ib, II-V. The HPLC retention times of three of these, G*-Ia, Ib and II, showed that they were identical with the adducts formed by tissue culture upon incubation with [^{3}H]DMBA, followed by isolation of RNA and hydrolysis to nucleosides and adducts. However, the three adducts constitute less than 10% of the total nucleoside /[^{3}H]DMBA adducts.

We have already shown that the full structures of G*-Ia and Ib can be represented as depicted in Fig. 9. Namely,DMBA is metabolized to the (5R,6S)-oxide which is trans-cleaved by the 2'-OH of guanosine (Refs.11,12). The structures of G* II-V are discussed in the following. The UV spectrum of the tissue culture product G*-II shown in Fig.10 was superimposable on that of the other three. Similarly, the CD spectra of II-V constituted two pairs having enantiomeric relations. These relations are most revealing since they show that the structures of II-V closely resemble each other, and that they can be divided into enantiomeric pairs.

Since the UV is dominated by the DMBA chromophore, the pK values of the guanine moiety cannot be obtained from it. However, advantage was taken of the intensely coupled CD curve which underwent changes as the electronic spectrum of the guanine portion changes with pH. Because of the great intensity of the split CD extrema, several μg's of sample suffice to measure the pKå' values (Refs.11,13;Fig.11). The presence of two dissociation constants immediately lead to the following three substitution patterns on

IN VITRO

DMBA-OXIDE AND GUANOSINE REACTED IN 2:1 ACETONE:WATER, pH 9.5

PRODUCTS SEPARATED BY LH-20, THEN HPLC ZORBAX-ODS
OR G-10, THEN HPLC μ-C_{18}

15% OF GUANOSINE REACTED

PRODUCTS: G*-IA > III > II > IB > IV > V

****

TISSUE CULTURE

TRITIATED DMBA INCUBATED WITH RAT LIVER CELLS

RNA, THEN ADDUCTS ISOLATED

G*-IA, IB AND II PRODUCED, 10% OF TOTAL ADDUCT

Fig.8. Formation of G*-Ia,etc.

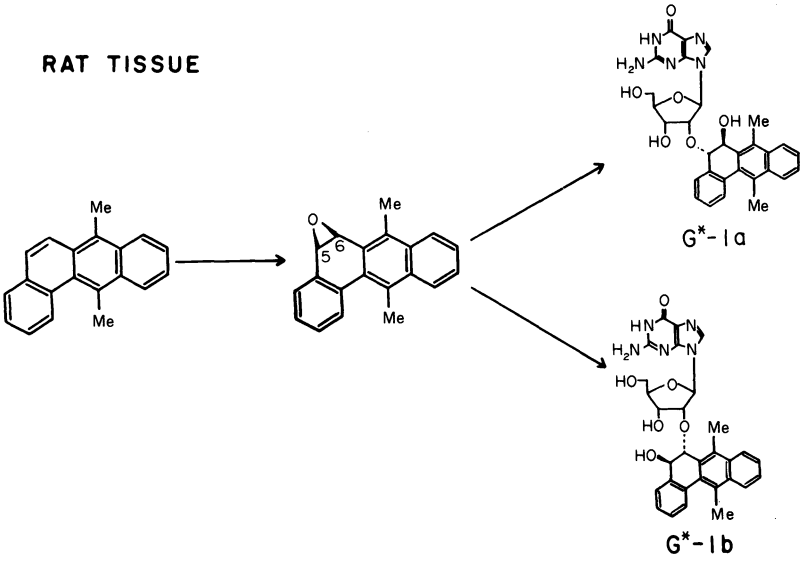

Fig.9. Tissue culture products, G*-Ia and -Ib.

the guanosine moiety: N^2, C-8 or the ribose. Although the N^2- substituted adducts (Ref.9) and ribose-2'-OH substituted adducts (Ref.11,12) had already been characterized earlier, this does not automatically lead to an adduct linked through C-8 since the oxirane does not necessarily open trans. However, it is hard to account for the production of four new closely related adducts other then a linkage through C-8.

The MS high-resolution was not diagnostic for offering positive evidence with respect to C-8 attachment since the high-mass region peaks were all derived from the hydrocarbon portion (Fig.12). However, after many futile attempts to obtain a peak containing the purine moiety, it was gratifying to

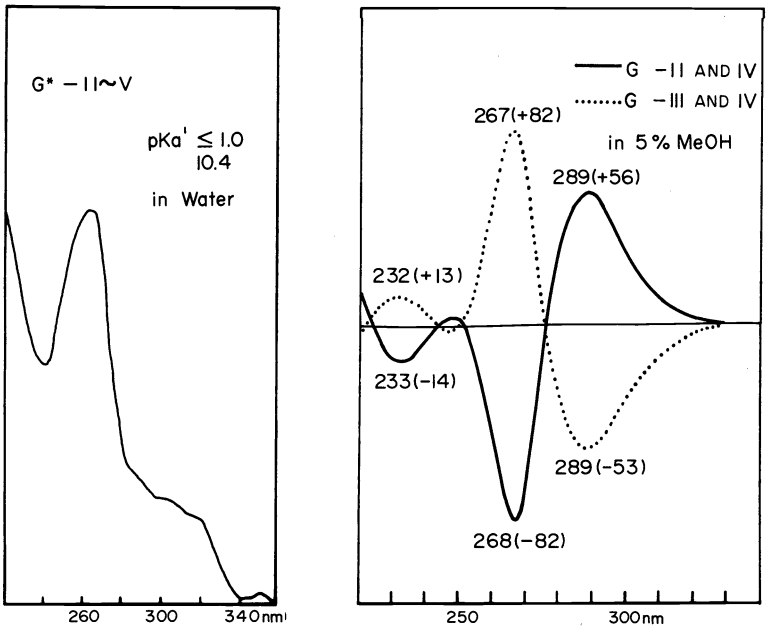

Fig.10. UV and CD of G*-II, III, IV and V.

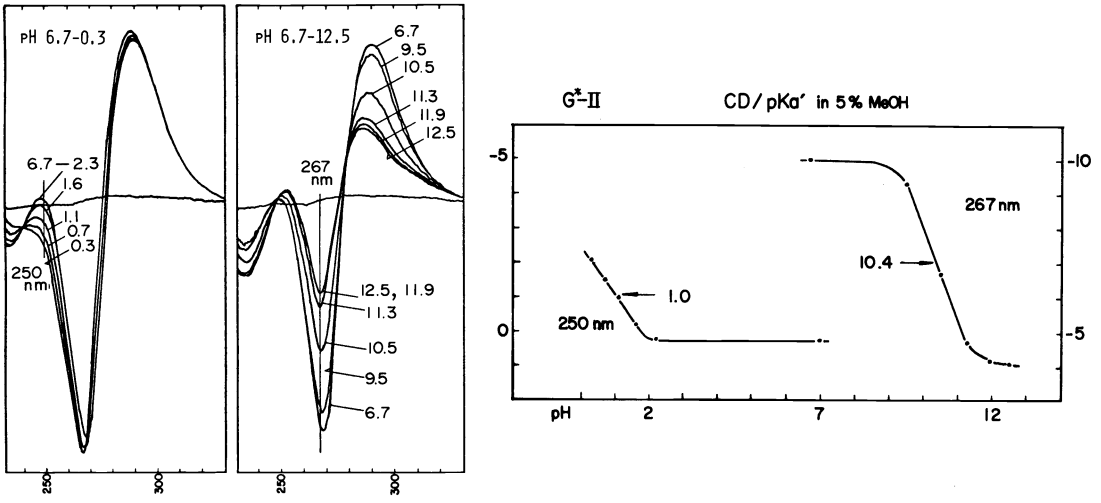

Fig.11. Apparent dissociation constant of G*-II from CD.

find that the high resolution El-MS of G*-II peracetate finally gave a peak at m/e 299, $C_{21}H_{17}NO$, which establishes that the DMBA moiety is linked to C-8. The fact that the pk_1' of adduct II, in contrast to the 2.2 value for guanosine, is lower than 1 is in accord with the presence of a bulky group at C-8 because this would favor deprotonation from the imidazole ring, or lowering of pK_1'.

It now remains to determine whether the guanosine is linked to C-5 or C-6 of the DMBA portion. The limited amount (ca. 0.5 mg of G*-II and III; quantities of G*-IV and V were too small for measurements), instability and poor solubility presented many difficulties in PMR measurements; they

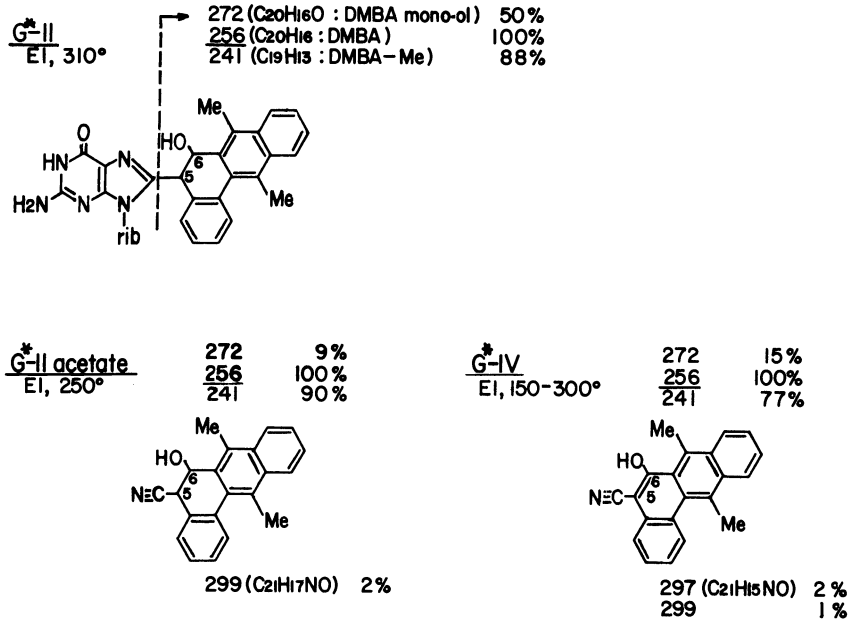

Fig.12. High-resolution MS data of G*-II and its acetate(Varian MAT731)

were finally measured in dry DMSO-d_6 in which the solvent peaks were removed by the inversion-recovery technique (Ref.14). The 5-H and 6-H chemical shifts will be discussed first. In the known cases of isomeric DMBA-guanosine N^2-adducts G-III and G-I (Ref.9) (Fig.13), the shifts of H-5 and H-6 are heavily dependent on whether the substituents are on C-5 or C-6. Namely, the carbinyl proton appears at 5.50 ppm in G-III but is at 5.07 ppm in G-I; similarly, the protons at the points of attachments of the guanosyl group are at 5.40 ppm in G-III but is at 5.82 ppm in G-I. It is seen that the 6-H signals are located ca. 0.4 ppm downfield than the corresponding 5-H signals. The same tendency is seen in the shifts of DMBA-5,6-oxide and in both the cis and trans DMBA-5,6-diols. The downfield shift of 6-H signals is attributed to the compression effect of the 7-Me group. In G*-II the two methine signals assignable to 5-H/6-H are at 4.80 and 6.20 ppm. The 4.80 ppm peak, in view of its high chemical shift, is due to the methine to which the

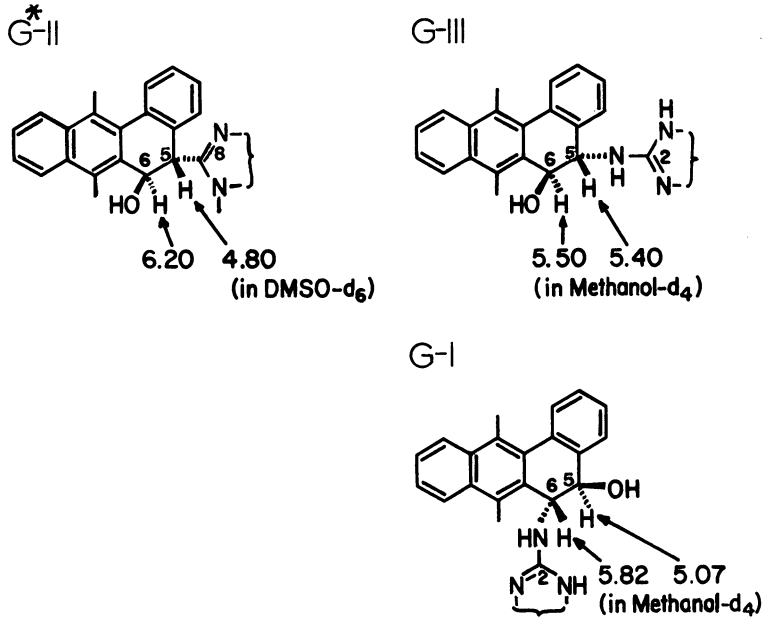

Fig.13. Some PMR data of G*-II, G-III and G-I.

guanosine C-8 is linked; the lower field 6.20 ppm peak represents the carbinyl proton. The low chemical shift of 6.20 indicates that the hydroxyl is at C-6 and not at C-5; if it were at C-5 it would be difficult to rationalize the difference between the 5.07 ppm value of G-I (in spite of the difference in solvent and the unknown effects of the purine ring current).

The point of linkage is supported by the following PMR data for G*-II and III (Fig.14), the CD of which are enantiomeric (Fig.10). All signals for II and III, including the 5-H, 6-H and 7-Me signals had identical or very similar chemical shifts except for 4-H, which was centered around 7.6 ppm in G*-II (hence overlapping with 1-H) but appeared as an isolated 1H multiplet at 7.4 ppm in G*-III. This single difference can be accounted for by the attachment of the guanosine residue at C-5 as follows. If the DMBA and purine nuclei of one isomer are represented by horizontal and vertical lines, and the ribose moiety by a hook (pointing forward from the paper face) as shown schematically in the bottom left drawing in Fig.14, it becomes clear that in the diastereomer in which the purine configuration is β, the ribose moiety now extends to the rear of the paper. Thus, depending on whether the guanosine configuration is α or β, the chiral ribose group exerts a different influence on 4-H (for steric reasons it is reasonable to assume the depicted conformation around the DMBA 5-C/guanosine 8-C bond,i.e., the ribose "exo" conformation). The attack of guanosine at C-5 is also preferred on steric grounds because of the 7-Me group.

The absolute configuration of the tissue culture product G*-II is as represented in Fig.14 because it is more likely to be derived from the same (5R,6S)-oxide shown in Fig. 9 rather than its enantiomer. The structure of the other major in vitro product G*-III then becomes 5β-guanosine/6α-OH; in view of the overlapping CD spectra of II and IV, and III and V (Fig.10), we propose the 5α-guanosine/6α-OH structure for IV and the 5β-guanosine/6β-OH structure for V, i.e., products of cis cleavage of the oxirane. In conclusion we have determined the structures of the three tissue culture products G*-Ia, Ib (Fig.9) and II (Fig.14). That these adducts, when produced in vitro, require slightly basic conditions (pH 9.5 in 50% aq. acetone) can be accounted for the facts that the 2'-OH is the most acidic of the ribosyl hydroxyl groups (Ref.15), and that under basic conditions the N^1-H is partly dissociated (pK_2 9.5) so that C-8 becomes a nucleophilic center (Ref.7).

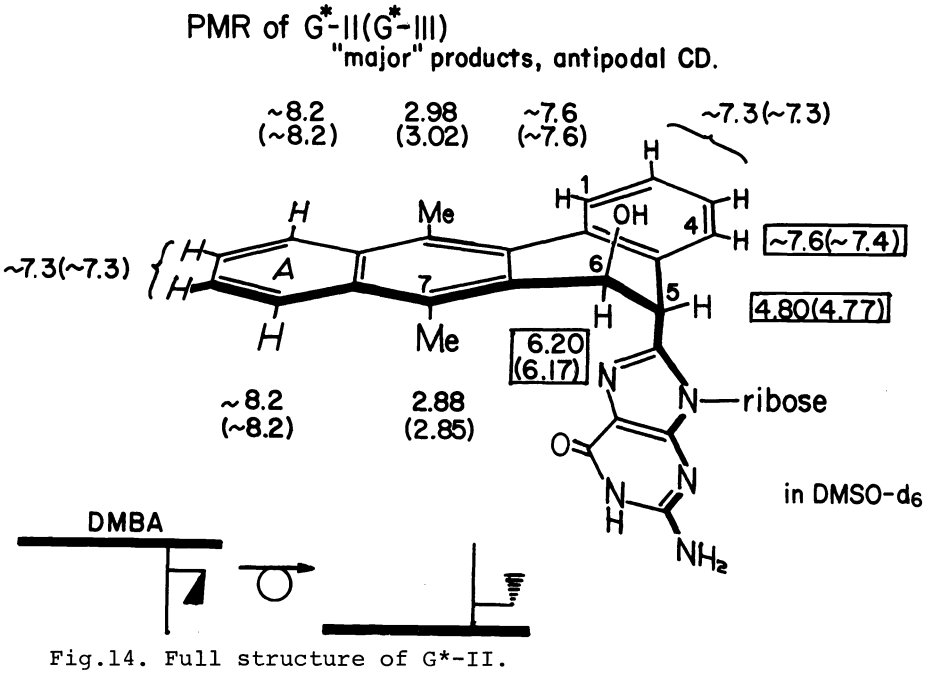

Fig.14. Full structure of G*-II.

3. Structure of neosaxitoxin, a sodium channel blocker (Ref.16).

The explosive growth of toxic dinoflagellates or occurrence of "bloom" leads to the so-called paralytic shellfish poisoning (PSP) as a result of these organisms infecting clams and some other marine animals. The most widespread and well-studied toxic dinoflagellates are the Pacific Gonyaulax catenella and the Atlantic G. tamarensis (Ref.17). The first member of the

new class of neurotoxins, saxitoxin (STX), was isolated in 1957 by Schantz and coworkers. After years of extensive structural studies by Rapoport's group, the structure was finally established by x-ray in 1975 by Schantz, Clardy and coworkers (Ref.18); it was independently confirmed also by x-ray

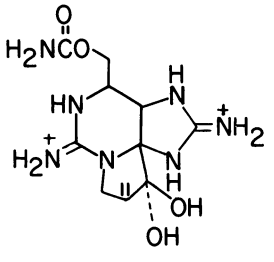

saxitoxin (STX)

Schantz, et al. JACS 97 1238 (1975)

Bordner, et al. JACS 98 5414 (1976)

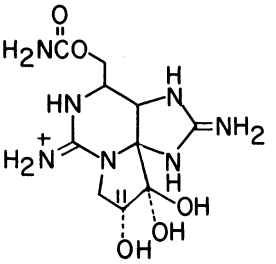

gonyautoxin (GTX)-II

GTX-III (II β-OH)

Shimizu, et al. JACS 98 5414 (1976)

Fig. 15. Saxitoxin and gonyautoxins-II and -III.

in 1976 by Rapoport and coworkers. The structures of two related toxins, gonyautoxin (GTX)-II and III, were elucidated by Shimizu et al. using a 1 mg hygroscopic mixture of the two toxins (Ref.20). Shimizu and coworkers are carrying out systematic studies of the distribution of dinoflagellate toxins in various sources and as a result have succeeded in isolating a variety of other related toxins after careful chromatographic separations (Ref.21). Like tetrodotoxin, the saxitoxins also block the sodium channels of membranes but have no effect on the potassium channels; the toxicity level is also similar, the LD_{50} of saxitoxin upon intraperitonial injection being 10 μg/kg with 20 g mice.

In the following we describe the results of structural studies on neosaxitoxin (neoSTX) which was first isolated as a minor toxin constituent in the toxic Alaska butter clam and later as a major toxin in the culture of Gonyaulax tamarensis (Ref.21). The toxicity of this neurotoxin is similar to that of STX, 1 mg of it being able to kill 5,000 mice each weighing 20 g. The spectroscopic and microchemical studies leading to the structure shown in Fig. 16 were carried out on a total of 2 mg of sample. The CMR signals of both STX and neoSTX were fully assigned by using the techniques of selective proton decoupling, gated undecoupled measurements, removal of solvent peaks by partial relaxed Fourier transform, etc. in a micro-CMR probe. The CMR spectrum of neoSTX in D_2O initially led to some confusion because: (i) unlike the 11-methylene in STX, which is fully deuterated only after 2 weeks, that of neoSTX was deuterated in about an hour, and consequently the C-11 only appeared as a weak signal due to the two D atoms: (ii) the appearance of only two sp^2 CMR peaks first led us to suspect that neoSTX was a decarbamoyl-STX. However, this was shown not to be the case by hydrolysis of neoSTX to decarbamoyl-STX. The presence of the carbamoyl group as well as two guanidium groups was finally shown by detection of three peaks at 157.4, 158.5 and 159.0 ppm in C_5D_5N containing a trace of D_2O.

The similarities in the CMR peak shifts between STX and neoSTX, except for C-6 and C-13, showed that the two had closely related structures. This was borne out by the PMR peaks which could be fully assigned by interrelating with the CMR data (Fig.17). Again it is clear that the most conspicuous differences are seen in the shifts of 6-H and the two 13-H's. These phenomena can be accounted for by placing a substituent on N-1. Thus the low-field shift of the C-6 doublet (64.4 vs. 53.2 ppm) and the high-field shift

of the C-5 doublet (56.9 vs.57.3 ppm) can be ascribed to β- and γ- effects, respectively. The shifts to lower fields of the 6-H and 13-H signals of neoSTX in comparison to STX can also be rationalized by the presence of an electronegative substituent on N-1. However, it was not immediately obvious what the N-1 substituent was. Being a marine product it could possibly have been a halogen as well as an OH group. In spite of numerous attempts at various modes of MS, it was not possible to obtain the M^+ peak. At one point, the possibility of elementary analysis by using all the remaining sample was considered, but this had to be abandoned because of expected ambiguities in the results.

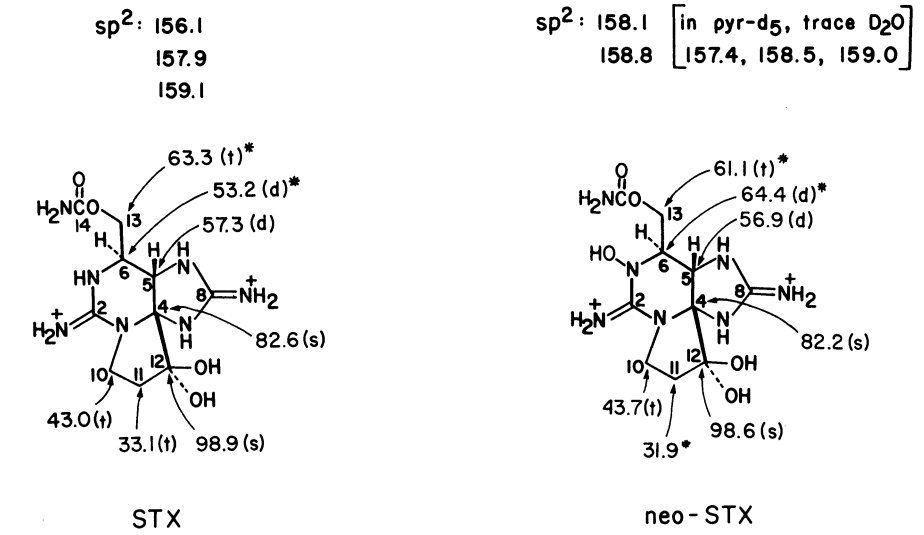

Fig.16. CMR data of STX and neo-STX

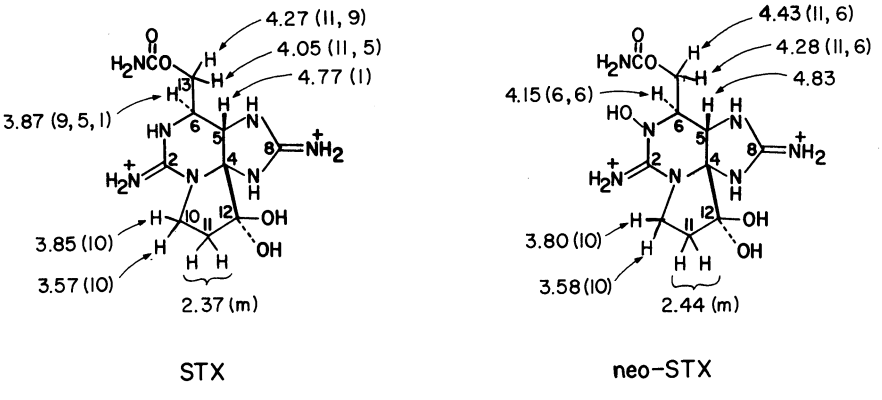

Fig.17. PMR data of STX and neo-STX

However, that the N-substituent was a dissociable hydroxyl group was established by microtitrations, which revealed the presence of three dissociable groups with pK_a values of 6.75, 8.65 and 11.65 (Fig.18); STX has only

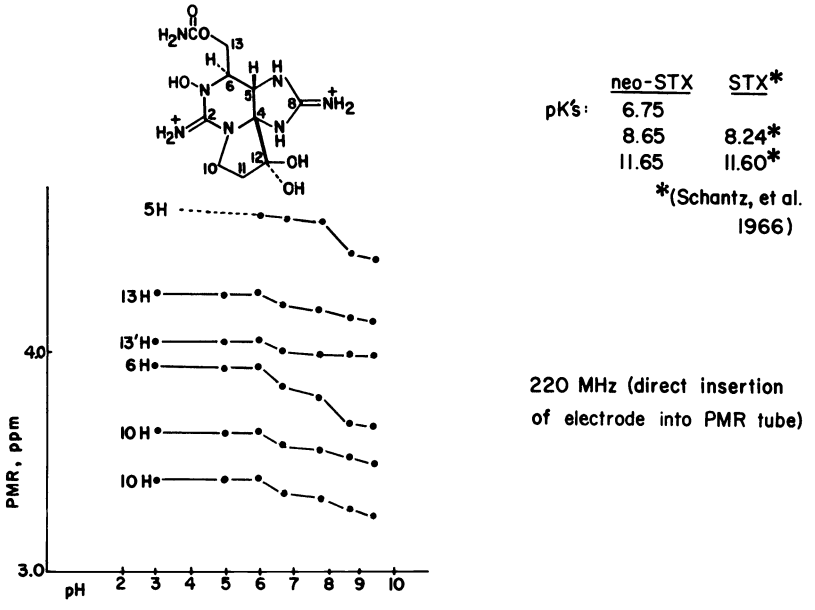

Fig.18. Change in PMR chemical shifts with pH.

two pK's at 8.24 and 11.60. The attachment of this extra OH to N-1 and not to N-9 was reflected clearly in the pH dependence of the PMR peaks of neoSTX which was measured by inserting a microelectrode directly into the PMR tube. As shown in Fig. 18, dissociation of the hydroxyl group at ca. pH 6.75 is accompanied by a shift to higher-field of the nearby 6-H; the 10-H's are also affected because the guanidium group becomes zwitterionic after dissociation of the OH. In contrast, the 5-H peak is not affected by the OH dissociation, but instead undergoes a high-field shift at around pH 8.65, or when the imidazole guanidium dissociates. We attribute this anomally low pK_a value to a twisted guanidium group. Namely, if the nitrogen (N-5 or N-9) lone pair electrons do not overlapwith the guanidium orbitals, the distorted nitrogen will exert its electronegative effect and lower the pK_a of the guanidium group.

GTX-II, -III, (Fig.15) and neoSTX which contain an extra hydroxyl group in comparison to STX are the major toxins in the toxic dinoflagellate G. tamarensis. However, in the softshell clam Mya arenaria the major toxin is STX. It is therefore conceivable that a biotransformation takes place in the shellfish which results in the loss of the extra hydroxyl group.

4. Mode of action of DBA, an antisickling agent (Ref.22)

Sickle cell anemia is a serious genetic disease which affects the black race (Ref.23). Hemoglobin, a protein with a molecular weight of 66,000 consists of two α-chains and two β-chains. The molecular defect of the homozygote SS sickle cell hemoglobin HbS occurs in the sixth amino acid residue from the amino terminal in the two β-chains; namely, in the β-chains of normal hemoglobin (HbA) it is glutamic acid whereas in HbS it is instead valine. A higher estimate of the homozygotes in USA is 54,000 (Ref.23a). At present there is no satisfactory treatment for this disease.

Deoxygenation of normal HbA does not lead to morphological changes. In contrast, deoxygenation of HbS by physical (exercise, bubbling nitrogen,etc.) or chemical (reduction) means transforms the normal round red blood cells (erythrocytes) into irregular sickle-shaped cells which are fragile, clots the vessels and impairs oxygen transport.

We reported the new antisickling and desickling agent DBA (3,4-dihydro--2,2-dimethyl-2H-1-benzopyran-6-butyric acid) which was modified after a natural product xanthoxylol, a constituent of the Nigerian tree Fagara xanthoxyloides (Ref.24). We reported that according to in vitro results it acted as an effective antisickling and desickling agent at the low

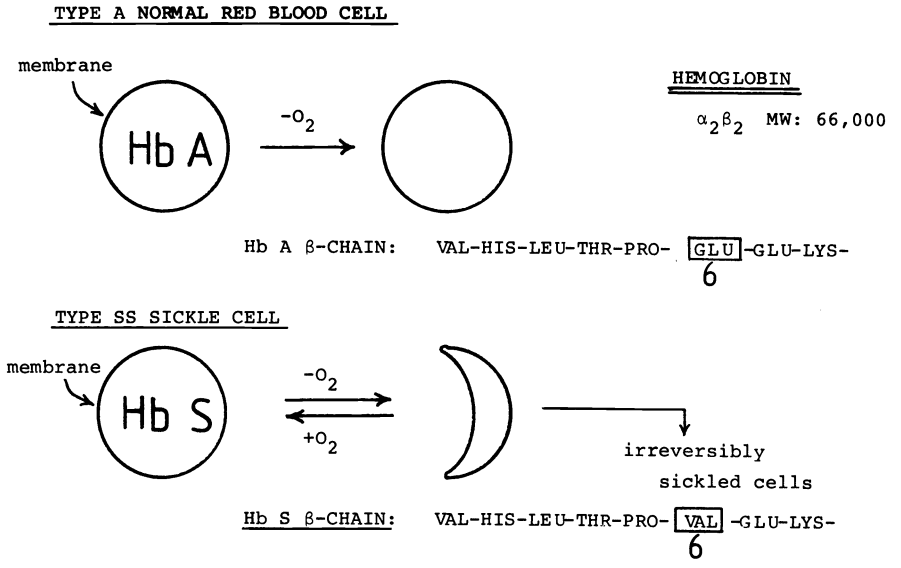

Fig.19. Type A and type SS blood cells.

concentration of ca. 3 mM and that it had no acute toxicity against male mice. However, no clinical studies have yet been carried out. DBA can be readily synthesized by Friedel-Crafts acylation of the benzopyran nucleus with

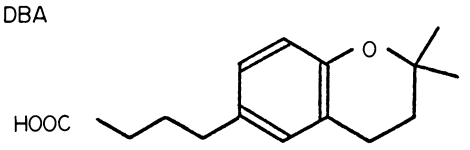

succinic anhydride followed by Clemmensen reduction. Usage of [1,14-^{14}C] succinic anhydride yields the ^{14}C-labeled DBA; it was shown by biosynthetic experiments with ^{14}C-DBA that the activity of DBA was not due to covalent modification of the β-chains but rather due to noncovalent binding to hemoglobin or interaction with the red cell membrane (Ref.24).

Subsequent experiments have shown that the mode of action of DBA can indeed be attributed to the displacement of membrane-bound β^S chains (defective β-chains) and inhibition of β^S and α-chains to stroma (membrane). The SS reticulocytes (young erythrocytes of homozygotes) were incubated for 1 hr. with ^{3}H-leucine and other cold amino acids (AA), and this was separated into two equal aliquots (Fig.21). The experimental erythrocytes were further incubated with cold AA and 3.8 mM DBA, washed, lysed with EDTA, and fractionated into the supernatant and stroma (membrane). The control was run similarly except that saline was added instead of DBA. Ater chromatography of the globin it was found the in comparison to the control, the supernatant contained 27% more whereas the stroma contained 30% less of β^S. These experiments demonstrate the displacement of stroma-bound β^S by DBA. Similar experiments with the bloods of six patients indicated that DBA inhibits the binding of both β^S and α-chains to the stroma by 4-56% at DBA concentrations of 0.2 to 3.8 mM (the effect of DBA depended more on the blood specimen rather than the DBA concentration).

In connection with these results, an important paper by Luer and Wong (Ref.25) has shown that the erythrocyte membrane protein of sickle cell anemia patients differ in structure from that of normal red blood cells. In view of this report, it is significant that DBA is an antisickline agent which acts on the red cell membrane and probably affects membrane-cytoskeletal interactions.

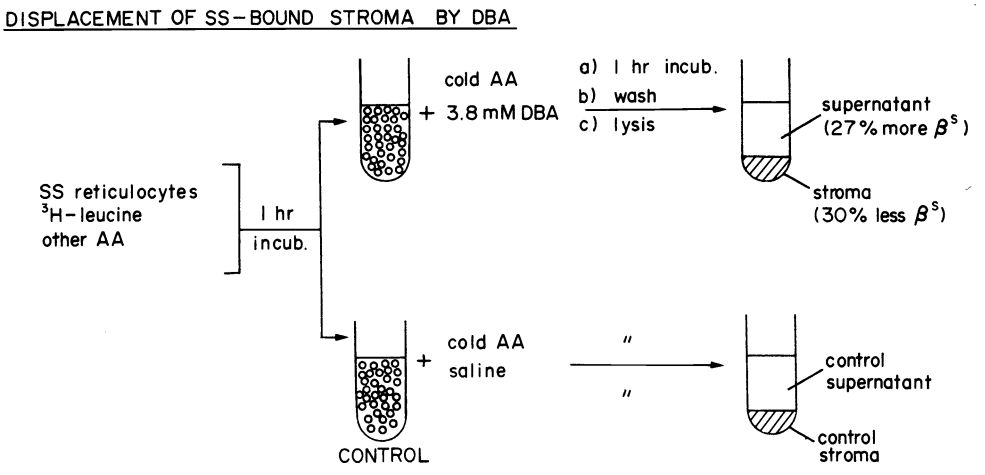

Fig.21. Displacement of SS-hemoglobin by DBA

Acknowledgement - All studies described here were carried out in collaboration with other institutions as follows: (1) mitotic hormone, Dr. D. Lynn (Chemistry) and Prof. L. Evans, Ms. S. Almeida (Manhattan College,Plant Morphogenesis Lab), Dr. S.L. Patt (Varian Associates), Dr. J. Occolowitz (Eli Lilly Co., MS measurements); (2) G*-II, Dr. H. Komura, Dr. H. Kasai, I. Miura (Chemistry) and Prof. D. Grunberger, Dr. K. Frenkel (Columbia Univ., College of Physicians and Surgeons); (3) neoSTX, I. Miura (Chemistry) and Prof. Y. Shimizu, Dr. C. P. Hsu (Univ. of Rhode Island,Pharmacognosy); (4) DBA, Dr. V. Balogh-Nair (Chemistry) and Prof. C. Natta (Columbia Univ.,College of Physicians and Surgeons). I am greatly indebted to my colleagues for the opportunity of carrying out these interdisciplinary studies. The work was suppored by NIH grants CA 11572, AI 10187 and NSF INT 76-10311.

REFERENCES

1. D. G. Lynn, K. Nakanishi, S. L. Patt, J. L. Occolowitz, S. Almeida and L. S. Evans, J.Am.Chem.Soc. in press; L. S. Evans, S. Almeida, D. G. Lynn and K. Nakanishi, Science in press.

2. W. S. Bullough, Biol.Rev. 37, 307 (1962).

3. J. C. Houck, ed. "Chalones", American Elsevier Publishing Co., New York, 1976.

4. L. S. Evans and J. Van't Hof, J.Exp.Cell.Res. 82, 471 (1973); 87, 259 (1974).

5. A. R. Katrizky, "Physical Methods in Heterocyclic Chemistry", Vol.II, Academic Press, New York, pp 274-303 (1963).

6. "Merck Index", 9th Edition, Merck & Co., Inc., Rahway, N.J., p.1243 (1976).

7. H. Komura, I. Miura, H. Kasai, K. Nakanishi, K. Frenkel and D. Grunberger, in preparation.

8. C.A.H. Bigger, J.E. Tomaszweski and D. Dipple, Biochem.Biophys. Res. Commun. 80 229 (1978); P. Vigny, H. Duquesne, H. Coulomb, B. Tierney, P. L. Gover and P. Sims, FEBS Lett. 82 278 (1977): D. M. Jerina, H. Yagi, M. Schaefer-Ridder, M. Lehr, D. R. Thakker, A.W. Wood, A.Y. H. Ryan, D. West, W. Levin and A. H. Conney, Cold Spring Harbor Symp. Origins of Human Cancer, 639 (1977).

9. A. M. Jeffrey, S. H. Blobstein, I. B. Weinstein, F. A. Beland, R. G. Harvey, K. Kasai and K. Nakanishi, Proc.Natl.Acad.Sci.USA 73 2311 (1976).

10. V. Ivanovic, N. E. Geacintov, A. M. Jeffrey, P. P. Fu, R. G. Harvey and I. B. Weinstein, Cancer Letters 4 131 (1978).

11. H. Kasai, K. Nakanishi, K. Frenkel and D. Grunberger, J.Am.Chem.Soc. 99 8500 (1977).

12. K. Nakanishi, IUPAC Congress, Tokyo, 1977; Pure & Applied Chem., in press.

13. H. Kasai, S. Traiman and K. Nakanishi, JCS Chem.Commun., in press.

14. A. M. Jeffrey, K. W. Jennette, S. H. Blobstein, I. B. Weinstein, F. A. Beland, R. G. Harvey, H. Kasai, I. Miura and K. Nakanishi, J.Am.Chem.Soc. 98, 5714 (1976).

15. For example, D. M. G. Martin, C. B. Reese and G. F. Stephenson, Biochem. 7, 1406 (1968).

16. Y. Shimizu, C. P. Hsu, I. Miura and K. Nakanishi, J.Am.Chem.Soc., in press.

17. For a review of dinoflagellate toxins see: Y. Shimizu in P. J. Scheuer ed., "Marine Natural Products", Academic Press, Vol.1, pp. 1-42 (1978).

18. E. J. Schantz, V. E. Ghazarossian, H. K. Schnoes, F. M. Strong, J. P. Springer, J. O. Pezzanite and J. Clardy, J.Am.Chem.Soc. 97, 1238 (1975).

19. J. Bordner, W. E. Thiessen, H.A. Bates and H. Rapoport, J.Am.Chem.Soc. 97, 6008 (1975).

20. Y. Shimizu, L. J. Buckley, M. Alam, Y. Oshima, W. E. Fallon, H. Kasai, I. Miura, V. P. Bullo and K. Nakanishi, J.Am.Chem.Soc. 98, 5414 (1976).

21. Y. Shimizu, M. Slam. Y. Oshima and W. E. Fallon, Biochem. Biophys.Res. Commun. 66, 731 (1975); Y. Oshima, L. J. Buckley, M. Slam and Y. Shimizu, Comp.Biochem.Physiol. 57, 31 (1977).

22. C. Natta, V. Balogh-Nair and K. Nakanishi, in preparation.

23. (a) H. Abramson, J. F. Bertles and D. L. Wethers, ed., "Sickle Cell Disease". Mosby, St. Louis, Missouri (1973); (b) Proc.1st Natn.Symp. Sickle Cell Disease, Washington, D.C., Dept. of Health, Education and Welfare Publication No. (NIH) 75-723 (1974).

24. D. E. V. Ekong, J. I. Okogun, V. U. Enyenhi, V. Balogh-Nair, K. Nakanishi and C. Natta, Nature 258, 743 (1975).

25. C. A. Luer and K-P. Wong, Biochem.Med. 19, 95 (1978).